Photosynthesis Research **22**: 233–246, 1989.

Regular paper

Spectral hole burning of the primary electron donor state of Photosystem I

J. Kevin Gillie[1], Paul A. Lyle[1], Gerald J. Small[1] & John H. Golbeck[2]
[1] *Ames Laboratory-USDOE and Dept. of Chemistry, Iowa State University, Ames, Iowa 50011, U.S.A.;*
[2] *Department of Chemistry, Portland State University, Portland, Oregon 97207, U.S.A.*

Received 13 March 1989; accepted in revised form 17 June 1989

Key words: Electron–phonon coupling, hole burning spectroscopy, Photosystem I

Abstract

Persistent photochemical hole burned profiles are reported for the primary electron donor state P700 of the reaction center of PS I. The hole profiles at 1.6 K for a wide range of burn wavelengths (λ_B) are broad (FWHM $\sim$ 310 cm^{-1}) and for the 45:1 enriched particles studied exhibit no sharp zero-phonon hole feature coincident with λ_B. The λ_B-dependent hole profiles are analyzed using the theory of Hayes et al. [J Phys Chem 1986, 90: 4928] for hole burning in the presence of arbitrarily strong linear electron–phonon coupling. A Huang–Rhys factor S in the range 4–6 and a corresponding mean phonon frequency in the range 35–50 cm^{-1} together with an inhomogeneous line broadening of $\sim$ 100 cm^{-1} are found to provide good agreement with experiment. The zero-point level of P700* is predicted to lie at $\sim$ 710 nm at 1.6 K with an absorption maximum at $\sim$ 702 nm. The hole spectra are discussed in the context of the hole spectra for the primary electron donor states of PS II and purple bacteria.

Abbreviations; NPHB – nonphotochemical hole burning, O.D. – optical density, PSBH – phonon sideband hole, PS I – Photosystem I P680, P700, P870, P960 – the primary electron donors of Photosystem II, Photosystem I, *Rhodobacter sphaeroides*, *Rhodopseudomonas viridis*, PED – primary electron donor, RC – reaction center, ZPH – zero-phonon holes

1. Introduction

Spectral hole burning (Moerner 1988) of chlorophyllic pigments of photosynthetic reaction centers (RC) (Meech et al. 1985, Boxer et al. 1986a, Boxer et al. 1986b, Meech et al. 1986, Gillie et al. 1987a, Tang et al. 1988, Tang et al. 1989, Jankowiak et al. 1989) and light harvesting (antenna) complexes (Gillie et al. 1987b, Köhler et al. 1988a, Köhler et al. 1988b, Renge et al. 1988, Gillie et al. 1989, Johnson and Small 1989) has been shown to be a useful probe of excited electronic structure and dynamics. For example, nonphotochemical hole burning (NPHB) has been used to determine the frequencies and Franck–Condon factors for 40 intramolecular modes of the Q_y state of Chl *a* in the light harvesting complex of Photosystem I (PS I) (Gillie et al. 1989). These and corresponding data for protein phonons were used to show that excitation transport within the core antenna complex is mediated by phonons ($\omega_m \sim 22\,cm^{-1}$) rather than intramolecular modes (Gillie et al. 1989). For both Chl *a* and *b* of the light harvesting complex (PSI-200) the linear electron–phonon coupling for the Q_y transition is weak (Huang–Rhys factor $S \approx 0.8$). As a consequence the low temperature absorption width of the Q_y transition is dominated by site inhomogeneous line broadening, Γ_I. Furthermore, the electronic structure and geometry of the Q_y state for Chl *a* and *b* suffer minimal perturbations from interactions with the protein or inter-pigment coupling (Gillie et al. 1989).

The NPHB spectra for antenna phycobilosomes

of *Masticogladus laminosus* (Köhler et al. 1988a, Köhler et al. 1988b) and BChl *a* of *Prosthecochloris aestuarii* (Johnson and Small 1989) are also characterized by weak electron–phonon coupling ($S \lesssim 1$). Thus, their short burn hole profiles, like those of PSI-200, are dominated by the zero-phonon hole (ZPH), with the broader one-phonon sideband holes relatively weak. This is also the case for the intrinsic accessory pigments of the RC of PS II (Jankowiak et al. 1989).

Such hole profiles provide a striking contrast with those observed for the primary electron donor (PED) states of PS I (P700*) (Gillie et al. 1987a), PS II (P680*) (Jankowiak et al. 1989), *Rhodopseudomonas viridis* (P960*) (Boxer et al. 1986b, Meech et al. 1986, Tang et al. 1988, Tang et al. 1989) and *Rhodobacter sphaeroides* (P870*) (Meech et al. 1985, Boxer et al. 1986a). Although the spectra for these PED states exhibit differences, which will be delineated later, they are dominated by a broad hole(s) with a width of a couple hundred cm^{-1}. When a relatively sharp (few cm^{-1}) ZPH is observed (Jankowiak et al. 1989, Tang et al. 1988, Tang et al. 1989), it appears as weak features at λ_B (burn wavelength) superimposed on a far more intense broad hole. The λ_B-dependence of the first reported hole profiles for P870 (Boxer et al. 1986a) and P960 (Boxer et al. 1986b) indicated that there is a significant homogeneous contribution to the width of the broad hole. The question of the origin of the homogeneous broadening has attracted considerable attention since it must reflect, in some way, the electronic structure of the PED state and its interactions with the protein and/or a close lying state(s) of the RC.

Two theories have been proposed for the large homogeneous broadening based on physical models proposed by Boxer et al. (1986b). The first theory proposed attributes the broadening to linear electron–phonon (either protein or inter-pigment) coupling and RC inhomogeniety (Hayes and Small 1986, Hayes et al. 1988), of a magnitude expected for a state that possesses significant charge-transfer character. An analytic expression for the hole profile, which is valid for arbitrarily strong coupling and large inhomogeneous broadening, was used (Hayes and Small 1986, Hayes et al. 1988) to account for the λ_B-dependence of the first reported hole spectra for P870 (Boxer et al. 1986a) and P960 (Boxer et al. 1986b). In this theory the homogeneous width of the broad hole reflects the width of the phonon progression which builds on the zero-phonon optical transition. The theory allows for the appearance of a ZPH superimposed on a broad hole provided the Huang–Rhys factor S is not too large [the Franck–Condon factor for the ZPH is roughly $\exp(-2S)$]. It is the width of the ZPH that would reflect electronic relaxation of the PED state (from its zero-point level). It should also be noted that if ω_m is the mean phonon frequency, $S\omega_m$ is the reorganization energy associated with the optical excitation ($2S\omega_m$ is the Stokes shift).

More recently, the ZPH has been observed for P870 (Johnson et al. accepted, Tang et al. accepted), P960 (Tange et al. 1988, Tang et al. 1989) and P680 (Jankowiak et al. 1989). Since in this paper we report on hole burning of P700, it is instructive to show here an example of the type of hole profile that has recently been reported for P680, Fig. 1. It is characterized by a relatively weak ZPH coincident with λ_B. To lower and higher energy of the ZPH are the pseudo-PSBH (phonon sideband hole) and real-PSBH displaced by $20\,cm^{-1}$ from the ZPH. This mean phonon frequency (ω_m) of $20\,cm^{-1}$ is in reasonable agreement with the value of $26\,cm^{-1}$ obtained using the measured Stokes shift for P680 and the relative intensity of the ZPH to the broad hole (Jankowiak et al. 1989). Satisfactory fits to the observed P680 profiles have been obtained (Jankowiak et al. 1989) using the theory of Hayes and Small (1986). The ZPH width has been used to determine a decay time for P680* (due to electron transfer) of 1.9 ± 0.2 ps at 1.6 K. This value can be compared with the value of 2.6 ± 0.6 ps at ice temperature (Wasielewski et al. 1989).

The second theory (Won and Friesner 1988a) shares certain features with the first, e.g., inhomogeneous broadening and linear electron-vibration coupling. But multiple modes (lower frequency monomer intramolecular and phonons) were introduced. In the application of the theory to the data for P870 (Boxer et al. 1986a) and P960 (Boxer et al. 1986b), weak electron-mode coupling was assumed for all modes (Won and Friesner 1988a). To explain the absence of ZPH in the hole spectra it was proposed that the PED state undergoes ultra-fast chaotic electronic decay due to strong coupling with some type of close lying charge-transfer state. This coupling ($\sim 200\,cm^{-1}$)

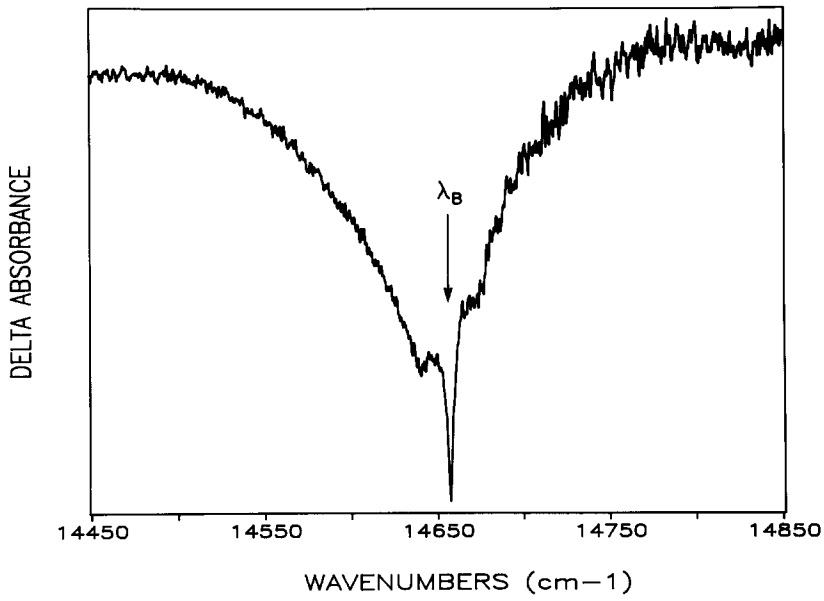

Fig. 1. Difference absorbance hole burned for P680 of the PS II reaction center. The spectrum was obtained for λ_B = 682.2 nm at T = 4.2 K with a read resolution of $\sim 0.1\,cm^{-1}$. The Δ-absorbance change at the peak is ~ 10%.

was shown to *eliminate all the ZPHs* predicted in its absence (Won and Friesner 1988a), as one might expect. The ZPHs include the one coincident with ω_B and the higher energy vibronic satellite holes (Small 1983). Based on the recently obtained data for the antenna Chl *a* and Chl *b* of PS I (Gillie et al. 1987b, Gillie et al. 1989), however, one would not expect to observe sharp vibronic satellite holes of any significant intensity since the *intramolecular* vibronic Franck–Condon factors are very small ($\lesssim 0.04$) and no excited state vibrations with a frequency less than $260\,cm^{-1}$ are active. The Franck–Condon factors for the low frequency intramolecular vibronic modes ($\lesssim 200\,cm^{-1}$) of the bacteriochlorophyll *a* in a glass at 5 K are estimated at $\lesssim 0.02$ based on fluorescence excitation spectra (Renge et al. 1987).

In this paper we report on the λ_B-dependence of the hole spectra for P700 of PS I. In an earlier paper the hole profile for enriched (35 antenna Chl *a*:P700) particles was shown to be dominated by a single broad hole carrying a width of $\sim 300\,cm^{-1}$ at 1.6 K (Gillie et al. 1987a). A weak but sharp ($\sim 0.05\,cm^{-1}$) ZPH coincident with ω_B was also observed (Gillie et al. 1987b). Here we present further evidence (Gillie et al. 1987b, Hayes et al. 1988) that this ZPH is not associated with photoactive P700. The spectra are interpreted using the theory of Hayes and Small (1986) and are discussed in the context of the hole spectra for the other PED states. A determination for the energy of the *zero-point* vibrational level of P700 at 1.6 K is made and a calculated absorption spectrum for P700 presented.

2. Experimental

PS I particles were isolated from spinach chloroplast and enriched to 45:1 Chl *a*:P700 via the procedure of Mullet et al. (Mullet et al. 1980). This particle contains the full set of electron acceptors A_0, A_1, F_x, F_A/F_B and a subset of the core antenna complexes (Golbeck 1987). It is devoid of the Chl *b*/Chl *a* light harvesting chlorophyll protein complex, LHCI. The Chl:P700 ratio was assayed by photo-oxidizing P700. The particles, suspended in a buffered glycerol/water (pH 8.0) mixture containing 0.1% Triton X-100, are stored at 77 K in the dark until needed.

For the experiments, the optical density of the samples was adjusted by dilution to the appropriate O.D. with a buffered (pH 8.3) glycerol/water (70:30) solution containing 100 mM Tris and 0.1%

Triton X-100. 1 mM ascorbic acid is added to prereduce P700. The samples were held in the dark at room temperature for a few minutes and then quickly cooled (< 5 min) to 4.2 K in a Janis Model 8-DT Super Vari-Temp liquid helium cryostat. All experiments were performed with the sample immersed in superfluid He at 1.6 K.

The spectra were measured in transmission with the output from a short arc 500 W xenon lamp (Canrad Hanovia 959C1980) dispersed by a 1.5 m Jobin–Yvon high resolution monochromator (model HR1500). The resolution for extended scans was $\sim 1\,cm^{-1}$. Data collection and monochromator were computer controlled. The burn laser was a Coherent 699-21 ring dye laser operating in the single frequency configuration and pumped with a 5 W argon ion laser. The laser linewidth was $\sim 0.002\,cm^{-1}$. The laser dye used was LD688 (Exciton) with a tuning range ~680–720 nm. Burn intensities were $< 10\,\mu W/cm^2$. Attempts to observe the ZPH coincident with ω_B included single frequency scanning over a 30 GHz range.

It should be noted that the photochemical hole burned spectra of P700 are persistent since the charged separated state $P700^+(F_A/F_B)^-$ is stable at liquid helium temperatures (Bearden and Malkin 1972, Ke et al. 1978).

3. Results

At 1.6 K the 45:1 PS I particles exhibit a principal absorption maximum near 670 nm due to Chl *a* of the core antenna complex and a distinct but weak shoulder located near 700 nm, which represents P700, upper curve of Fig. 2. The three lower absorbance spectra correspond to burns of 1, 5 and 10 min with $I_B = 5\,\mu W/cm^2$ and $\lambda_B = 701.8$ nm. No ZPH could be observed coincident with this λ_B-value or several other values in the range between 701 and 715 nm. Under comparable burning conditions and read resolution, the earlier studied 35:1 particles exhibited a readily discernible, albeit weak, ZPH coincident with λ_B. From Fig. 2 it is apparent that the P700 hole is broad (Δ OD spectra are shown later).

The increase in absorption to higher energy of ~700 nm seen in the upper spectrum of Fig. 2 is due to the onset of the Chl *a* antenna absorption. Figure 3 shows a series of hole burned spectra obtained with $\lambda_B = 693.2$ nm (the upper spectrum is the pre-burn absorption spectrum). At this wavelength absorption by the core antenna complex is dominant but there is some absorption due to the high energy side of the P700 absorption profile. The second and third curves of Fig. 3 are the hole burned spectra obtained with $I_B = 5\,\mu W/$

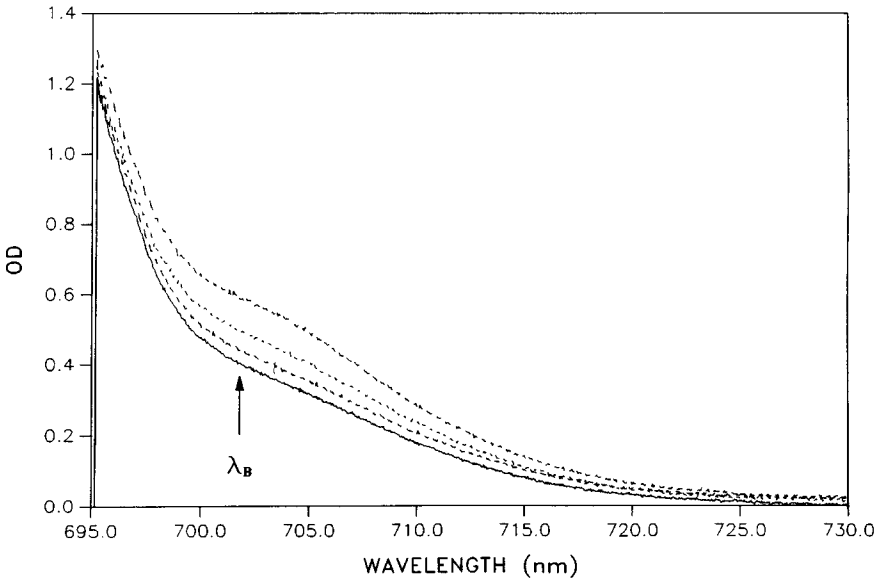

Fig. 2. Burn time dependence of the P700 bleaching at 1.6 K for 45:1 PS I particles, $\lambda_B = 701.8$ nm, $T = 1.6$ K. The top curve is the preburn spectrum. Burn times (second to fourth spectrum) are 1, 5, 10 min with burn intensity $I_B = 5\,\mu W/cm^2$.

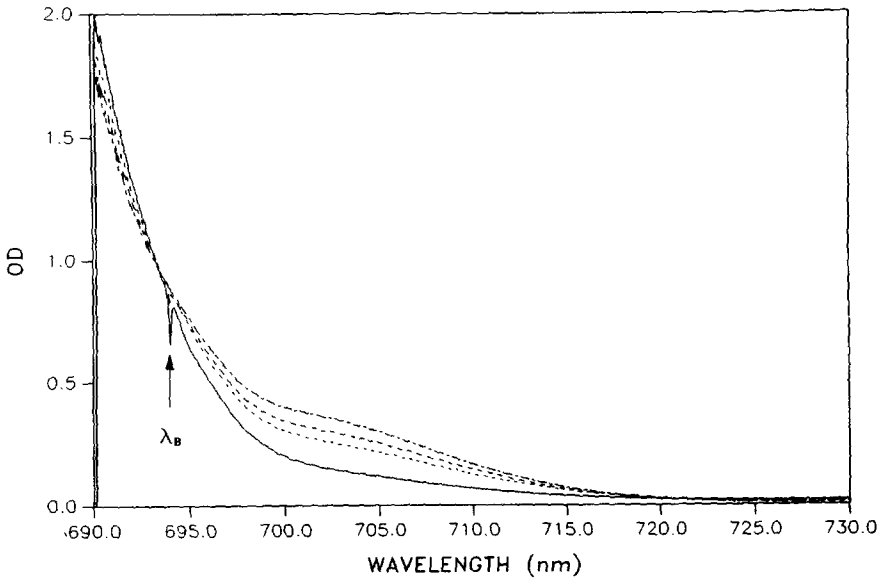

Fig. 3. Burn time dependence of the P700 bleaching for 45:1 particles, λ_B = 693.2 nm, T = 1.6 K. The upper spectrum is the preburn spectrum. Burn times for the second and third spectra are 1 and 10 min, respectively, with I_B = 5 μW/cm^2. The lowest spectrum was obtained by an additional 5 min burn with I_B = 2 W/cm^2. The ZPH is ascribed to NPHB of the antenna Ch *a*, see text.

cm^2 for burn times of 1 and 10 min. Although not apparent from the figure, a weak ZPH is observed for the 10 min burn. The lowest spectrum of Fig. 3 was obtained after an additional 5 min burn with I_B = 2 W/cm^2 and clearly shows a ZPH coincident with λ_B. The ZPH is ascribed to NPHB of the antenna Chl *a* (Gillie et al. 1987b, Gillie et al. 1989) and not P700 since the ZPH could not be observed for λ_B-values selective for P700. Although excitation transport within the core antenna complex is significantly slower at 1.6 K than at room T, the quantum efficiency for excitation trapping by P700 is still close to unity (Gillie et al. 1989). On the other hand, the NPHB quantum efficiency for the antenna Chl *a* is significantly less than unity (Jankowiak and Small 1987a, Jankowiak et al. 1987b). This explains why the ZPH develops at higher burn fluences than the P700 hole.

Figure 4 shows the ΔOD hole burned spectrum obtained with λ_B = 680.5 nm, which is close to the maximum of the antenna Chl *a* absorption at 670 nm. At 680.5 nm the P700 absorption is negligible. The *saturated* ZPH at λ_B, due to NPHB of antenna Chl *a*, is intense and accompanied by the real- and pseudo-PSBH (displaced by $\omega_m \sim 20$ cm^{-1}) (Gillie et al. 1987b, Gillie et al. 1989). The broad positive going feature at $\sim$675 nm is the anti-hole associated with NPHB (Gillie et al. 1989). The increase in noise in the vicinity of the anti-hole is due to the high O.D. near the absorption maximum. The broad P700 hole, produced by trapping of the antenna excitation, is also evident in the figure with a maximum near 702 nm.

The P700 ΔOD hole profiles obtained for λ_B = 715.0 and 706.5 nm are shown in Fig. 5 and the profile for λ_B = 702.6 nm in Fig. 6. The absorption by the antenna Chl *a* at these wavelengths is weak in comparison to P700. The maxima of the P700 holes for λ_B = 715.0, 706.5 and 702.6 nm are located at 705, 703 and 702 nm, respectively, and, again, no sharp ZPH is observed coincident with λ_B. The solid curves are fits to the spectra obtained using the theory of Hayes and Small (1986).

Before discussing the theoretical fits a brief overview of the theory is in order. The low temperature absorption profile due to a *single* absorbing site is written as (Hayes et al. 1988)

$$L(\Omega - \nu) = e^{-S} I_0(\Omega - \nu) + \sum_{r=1}^{\infty} \frac{S^r e^{-S}}{r!} I_r(\Omega - \nu - r\omega_m), \quad (1)$$

where ν is the zero-phonon transition frequency

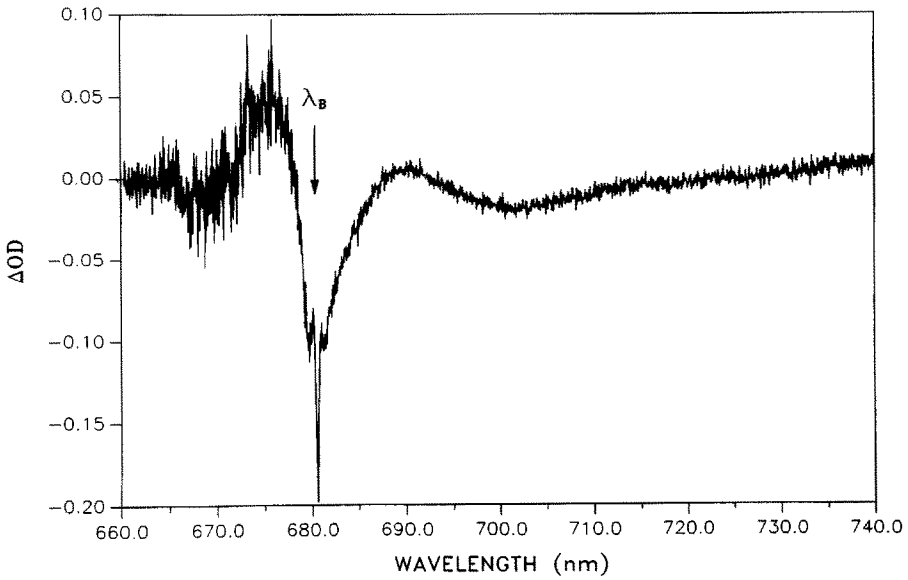

Fig. 4. Difference absorbance (ΔOD) hole burned spectrum of P700 for 45:1 particles, $\lambda_B = 680.5$ nm, $T = 1.6$ K. Excitation was for 10 min with $I_B = 50\,\mu W/cm^2$. The ZPH at λ_B and phonon sideband holes displaced from λ_B by $\sim 20\,cm^{-1}$ are due to NPHB, see text. The broad hole centered at ~ 702 nm is due to bleaching of the P700 absorption profile. For the spectrum shown here, *saturation* of the ZPH and phonon sideband holes gives the false impression that the linear electron–phonon coupling is stronger than reported earlier for antenna Chl *a* (Gillie et al. 1989). The increase in noise in the anti-hole region near 675 nm is due to the high O.D. of the sample near the absorption maximum (~ 670 nm).

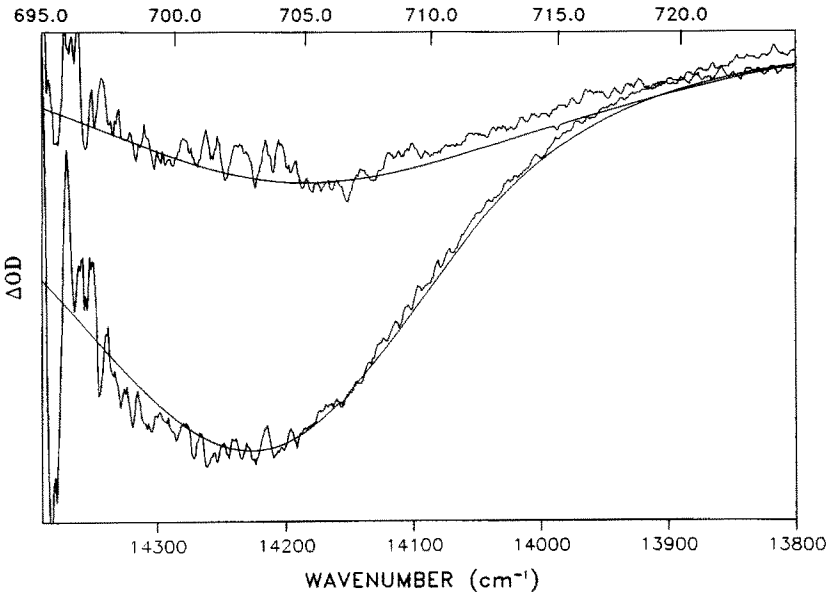

Fig. 5. Difference absorbance hole burned spectra of P700 for 45:1 particles, $\lambda_B = 715.0$ nm and $= 706.2$ nm (top and bottom, respectively), $T = 1.6$ K. The ΔOD scale is 0.2. Burn time was 30 s with $I_B = 10\,\mu W/cm^2$. The solid lines are computed fits with $S = 4.5$, $\omega_m = 45\,cm^{-1}$, $\Gamma_l = 100\,cm^{-1}$, $\gamma = 1\,cm^{-1}$, and $\nu_m = 14085\,cm^{-1}$. The calculated spectrum for $\lambda_B = 715$ nm exhibits a very weak ZPH which could not be expected to be observable given the signal to noise ratio of the experimental spectrum. The top ordinate scale is wavelength (nm).

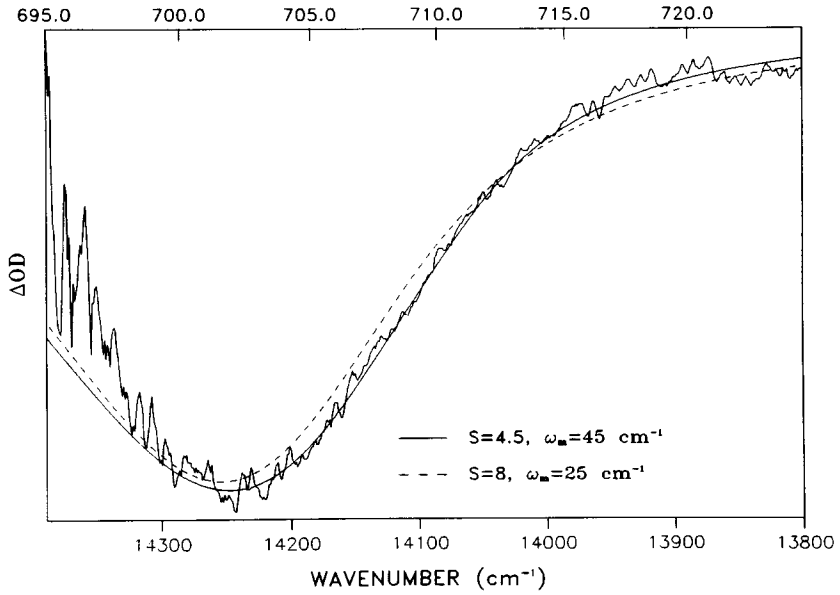

Fig. 6. Difference absorbance hole burned spectrum of P700 for 45:1 particles, $\lambda_B = 702.6$ nm, $T = 1.6$ K. The ΔOD scale is 0.2. Burn time was 30 s with $I_B = 10\,\mu W/cm^2$. The solid and broken lines are computed fits with $S = 4.5$ and $\omega_m = 45\,cm^{-1}$ (——) or $S = 8$ and $\omega_m = 25\,cm^{-1}$ (– – –). See Fig. 5 caption for other parameter values. The top ordinate scale is wavelength (nm).

and ω_m is the mean frequency for phonons which couple to the electronic transition. The Huang–Rhys factors is S and the Franck–Condon factors for the $r = 0, 1, \ldots$ phonon transitions are governed by the Poisson distribution $\{S^r e^{-S}/r!\}_r$. Thus, the Franck–Condon factor for the zero-phonon transition is $\exp(-S)$; its profile is a Lorentzian (l_0) with a FWHM = γ, which is the homogeneous linewidth of the zero-phonon line. The lineshape for the one-phonon profile is l_1 and is centered at $\nu + \omega_m$ with a FWHM of Γ. It is well known that the one-phonon profiles for electronic transitions of molecules imbedded in amorphous solids carry a width of about $30\,cm^{-1}$ and the profiles for antenna Chl *a* and *b* are no exception (Gillie et al. 1989). To a good approximation the profile can be taken to be a Gaussian. Equation (1) is valid for coupling to a pseudo-localized phonon or a distribution of host phonons governed by a suitable density of states. For the latter case and a one-phonon profile governed by a Gaussian, the width of the r-phonon profile (centered at $\nu + r\omega_m$) is given by $\Gamma_r = r^{1/2}\Gamma$ (Hayes et al. 1988). In order to derive an analytic expression for the hole profile, Lorentzians for l_r ($r \geqslant 1$) were used (Hayes and Small 1986) with widths governed by the Gaussian values, i.e., $r^{1/2}\Gamma$. Since that work it has been shown that the differences in the hole spectra calculated with Lorentzians and Gaussians are negligibly small (Lee et al. accepted). One further point is that the mean phonon frequency approximation for monomer electronic transitions in disordered hosts such as glasses, polymers (Hayes and Small 1978, Friedrich et al. 1980, Fearey et al. 1983, Small 1983, Friedrich and Haarer 1984), and proteins (Gillie et al. 1987b, Gillie et al. 1989) is an excellent one. We are not aware of a single example which indicates otherwise. Mixed crystal spectra do sometimes show sharp phonon structure due to pseudo-localized modes (Small 1970); this appears not to be the case for glassy hosts.

For amorphous hosts a Gaussian distribution for the disorder-induced distribution of zero-phonon transition frequencies is appropriate but, for the reason given above, a Lorentzian centered at ν_m with a width of Γ_I is employed and denoted by $N_0(\nu - \nu_m)/N$, where N is the total number of absorbing sites. Recent calculations have shown that the error introduced by utilization of a Lorentzian is small for the hole profile (Lee et al. accepted). Let the absorption cross-section, laser intensity and

photochemical quantum yield equal σ, I and ϕ, respectively. Then following a burn for time τ

$$N_\tau(\nu - \nu_m) = N_0(\nu - \nu_m)e^{-\sigma I\tau L(\omega_B - \nu)} \quad (2)$$

where ω_B is the laser burn frequency and $L(\omega_B - \nu)$ is given by Eqn. (1). To obtain the absorption spectrum, A_τ, following the burn we must convolve Eqn. (2) with $L(\Omega - \nu)$ and integrate over ν. Thus,

$$A_\tau(\Omega) = \sum_{r=0} \frac{S^r e^{-S}}{r!} \int d\nu\, N_0(\nu - \nu_m) e^{-\sigma I\phi\tau L(\omega_B - \nu)} \times l_r(\Omega - \nu - r\omega_m). \quad (3)$$

For simplicity the short-burn-time limit is employed so that the exponential can be expanded as $1 - \sigma I\phi\tau L(\omega_B - \nu)$. This approximation need not be made, although the resulting expressions are very cumbersome if it is not. The hole spectrum in the short-burn-time limit is simply

$$A_0(\Omega) - A_\tau(\Omega) = \sigma I\phi\tau \sum_{r,r'=0}^{\infty} \left(\frac{e^{-S}S^r}{r!}\right)\left(\frac{e^{-S}S^{r'}}{r'!}\right) \times \int d\nu\, N_0(\nu - \nu_m) l_r(\Omega - \nu - r\omega_m) l_{r'} \times (\omega_B - \nu - r'\omega_m). \quad (4)$$

Because we are interested in holes whose widths are comparable to Γ_I we cannot assume that $N_0(\nu - \nu_m)$ is constant in Eqn. (4). Integration of Eqn. (4) yields

$$[A_0 - A_\tau](\Omega) = \frac{\sigma\phi\tau}{3(2\pi)^2}\left(\sum_{r,r'=0}^{\infty} \frac{S^r e^{-S}}{r!}\frac{S^{r'}e^{-S}}{r'!}\right) \times \left[\left\{\frac{\Gamma_I + \Gamma_r}{(\Omega - \nu_m - r\omega_m)^2 + \left(\frac{\Gamma_I + \Gamma_r}{2}\right)^2}\right\} \times \left\{\frac{\Gamma_r + \Gamma_{r'}}{[\Omega - \omega_B + \omega_m(r' - r)]^2 + \left(\frac{\Gamma_r + \Gamma_{r'}}{2}\right)^2}\right\} + \left\{\frac{\Gamma_I + \Gamma_{r'}}{(\omega_B - \nu_m - r'\omega_m)^2 + \left(\frac{\Gamma_I + \Gamma_{r'}}{2}\right)^2}\right\} \times \left\{\frac{\Gamma_I + \Gamma_r}{(\Omega - \nu_m - r\omega_m)^2 + \left(\frac{\Gamma_I + \Gamma_r}{2}\right)^2}\right\}\right]. \quad (5)$$

The qualitative implications of Eqn. (5) are discussed by Hayes et al. (1988). Model calculations with realistic values for Γ, ω_m, γ and Γ_I are given in the same paper for various values of S ranging from 0.5 (weak coupling) to 8.0 (strong coupling). In Eqn. (5), $\Gamma_0 = \gamma$ and $\Gamma_r = r^{1/2}\Gamma$ ($r \geqslant 1$). For strong coupling ($S \gtrsim 2$) and $\omega_B \sim \nu_m$, the intensity of the ZPH relative to the broad hole is to a good approximation given by $\exp(-2S)$. For this value of ω_m, the ZPH is located near the center of the broad and more intense hole upon which it is superimposed. For $\Gamma_I \gtrsim S\omega_m$ a burn with ω_B located on the low and high energy sides of the absorption profile produce broad hole profiles that are shifted to the blue and red, respectively, of ω_B. Such behavior was observed by Boxer et al. (Boxer et al. 1986a) in their studies of P870 in polyvinyl alcohol films. On the other hand for P960, which exhibits a smaller value of Γ_I (for the samples employed), the broad hole maximum is quite insensitive to ω_B (Boxer et al. 1986b). For a fixed value of $S\omega_m$ increasing ω_m has the effect of producing a sharper drop-off in the wings of the hole. This is apparent from the two calculated curves in Fig. 6.

Application of the theory to the hole profiles of P700 is more difficult than for the other PED states, e.g., P680, since resolved phonon structure and the ZPH are not observed. Furthermore, the Stokes shift associated with P700 emission ($\sim 2S\omega_m$) is not known. However, we can estimate that $S \gtrsim 4.5$. Otherwise, a ZPH coincident with ω_B should have been observed (given the signal/noise ratio of our spectra) for $\gamma = 1\,\text{cm}^{-1}$. This value of γ corre-

sponds to the lifetime of P700 determined at ice temperature (Owens et al. 1987). If this lifetime were to decrease by a factor of about 2 in the low temperature limit, which is a possibility given the data for P870 (Martin et al. 1986, Breton et al. 1988), P960 (Breton et al. 1988) and P680 (Jankowiak et al. 1989, Wasielewski et al. 1989), a value of S closer to 4 would preclude observation of the ZPH in our spectra for PSI-45. In our earlier work with PSI-35 particles (Gillie et al. 1987a) a value of $S = 5.5$ was used to fit the hole spectra of P700 because the observed ZPH with a width of only $\sim 0.05\,cm^{-1}$ was assumed to be due to P700. The present and other (Gillie et al. 1987b, Hayes et al. 1988) studies indicate that it is not, *vide infra*.

The modest λ_B-dependence of the P700 hole profile maxima shown here, as well as that measured from $\lambda_B = 708.2$, 701.8 and 693.2 nm spectra, indicate that $\Gamma_I < S\omega_m$. The hole maxima for these three λ_B values are located at 703, 702 and 701 nm, respectively. One is constrained in the choice of the center (ν_m) of the zero-phonon transition frequency distribution by the observed λ_B-dependence (Hayes and Small 1986, Hayes et al. 1988) and the requirement that the calculated absorption spectrum must provide agreement with the observed spectrum.* The calculated hole profiles in Figs. 5 and 6 for $S = 4.5$, $\omega_m = 45\,cm^{-1}$, $\Gamma_I = 100\,cm^{-1}$, $\Gamma = 60\,cm^{-1}$ and $\nu_m = 14085\,cm^{-1}$ (710 nm) provide reasonable agreement with the observed profiles. The deviations on the high energy side of the hole maxima are the result of the appearance of an increase in absorption [with a maximum near 690 nm (Schaffernicht and Junge 1981, Sétif et al. 1984, Gillie et al. 1987a)] which has been attributed to an electrochromic shift of the Chl *a* associated with the primary acceptor A_0 of the RC and/or antenna Chl *a* in the near proximity of the RC (Schaffernicht and Junge 1981, Sétif et al. 1984). Thus, the quality of fit of the theoretical profiles can only be judged on the basis of the region of the experimental profiles in the vicinity of the hole maximum and to lower energy of the maximum. The P700 absorption spectrum calculated with the above parameter values is shown in Fig. 7. The calculated profile exhibits a maximum at 701.5 nm and a width of $350\,cm^{-1}$. From the theory one expects (Hayes et al. 1988) that the calculated absorption width should be given roughly by $S\omega_m + \Gamma_I$ ($300\,cm^{-1}$ in this instance).

* It has been stated (Won and Friesner 1988a, b) that the theory of Hayes and Small (1986) as applied to P870 and P960 (Hayes et al. 1988) yields incorrect absorption profiles. This statement is now acknowledged as being incorrect (Won and Friesner 1989).

4. Discussion

Chemical and white light bleaching experiments on PSI-35 particles discussed by Gillie et al. (1987b) and Hayes et al. (1988) had indicated that the sharp ZPH reported earlier (Gillie et al. 1987a) for P700 of PSI-35 particles is not due to photoactive P700. The present results for PSI-45 particles confirm this. With the procedure described by Golbeck (Golbeck 1980) we have found that an enrichment of $\sim 35{:}1$ is more difficult to attain than an enrichment of $\sim 45{:}1$. This suggests, perhaps, that the 35:1 particles could be subject to a higher probability for damage than the 45:1 particles. The sharp but weak ZPH reported for 35:1 particles could be due to inactive P700 or antenna Chl *a* perturbed by the isolation procedure. In any event, a hole width of $0.05\,cm^{-1}$ (Gillie et al. 1987b) translates to a minimum depopulation decay time for P700 at 1.6 K of 210 ps, which is difficult to reconcile in view of the measured decay times at room T (Fenton et al. 1979, Owens et al. 1987, Wasielewski et al. 1987) and the fact that the decay rates for P870* (Martin et al. 1986, Breton et al. 1988), P960* (Breton et al. 1988) and P680* (Jankowiak et al. 1989, Wasielewski et al. 1989) increase as the temperature is decreased from room T.

Turning now to the application of the theory to the ΔOD spectra shown in Figs. 5 and 6 it can be seen that the parameter values $S = 4.5$, $\omega_m = 45\,cm^{-1}$, $\Gamma = 60\,cm^{-1}$, $\Gamma_I = 100\,cm^{-1}$ and $\nu_m = 14085\,cm^{-1}$ provide reasonable fits to the observed profiles. In fitting to the spectra, Γ was held constant at $60\,cm^{-1}$, a value that is about twice that observed for the antenna Chl *a* (Gillie et al. 1989). The increase in Γ was scaled according to the ratio of the ω_m value utilized for P700 to that observed for the antenna Chl *a*. We hasten to add that comparable theoretical fits to the P700 hole profiles could be achieved using two or more mean phonon frequencies. However, "multi-phonon" fits

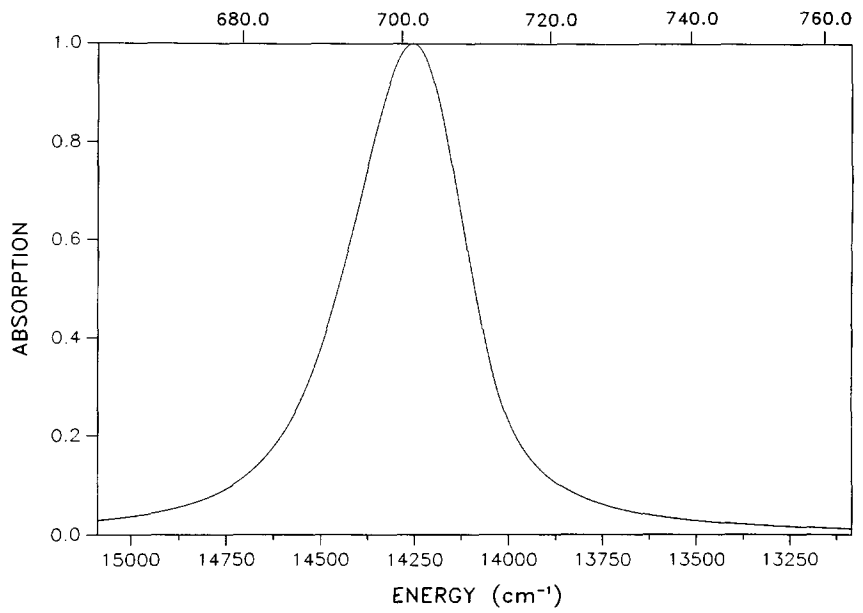

Fig. 7. Calculated absorption profile for P700 at 1.6 K. The parameters used were $S = 4.5$, $\omega_m = 45\,cm^{-1}$, $\Gamma_I = 100\,cm^{-1}$, $\Gamma = 60\,cm^{-1}$, $\gamma = 1\,cm^{-1}$ and $\nu_m = 14085\,cm^{-1}$ (710 nm).

are not justified at this time since underlying structure for P700 has not been observed. It was found that the λ_B-dependence of the hole maximum could not be accounted for if ν_m ($\lambda = 710$ nm) was varied by more than ± 2 nm from 710 nm. The fitting of the λ_B-dependence also depends quite sensitively on the ratio of $S\omega_m\Gamma_I$ as one would expect since in the limit $S\omega_m \gg \Gamma_I$ there should be no λ_B-dependence in the first approximation (Hayes et al. 1988). Comparable fits to the hole spectra can be obtained by increasing Γ_I somewhat [e.g., to $120\,cm^{-1}$ as determined for P680 (Jankowiak et al. 1989)] provided $S\omega_m$ is appropriately increased. This is also true if S is increased and ω_m decreased proportionately (for a fixed Γ_I). However, it was found that the goodness of fit to the low energy side of the hole profiles worsens if S is increased too much above 4.5, e.g., to 8 (Fig. 6). Our many calculations (only a few of which are shown here) indicate that S and ω_m values in the ranges 4–6 and 50–35 cm^{-1} and $\Gamma_I \approx 100\,cm^{-1}$ and $\nu_m = 14085\,cm^{-1}$ can adequately account for the observed hole profiles. The calculated absorption spectrum in Fig. 7 is difficult to compare with experiment because of interference by the low energy tail of the antenna Chl *a*, see upper curve of Fig. 2. However, since the homogeneous contribution to the P700 absorption is large the photochemical hole burning can produce a bleach that essentially encompasses the entire absorption profile. In particular, for λ_B significantly to the blue of 710 nm (center of the zero-phonon excitation frequency distribution), e.g., 702.6 nm as in Fig. 6, or located in the antenna Chl *a* absorption origin (Fig. 4) the hole should be a faithful representation of the P700 absorption profile at 1.6 K. The calculated absorption spectrum is in good agreement with the two hole burned spectra just mentioned. Thus, we conclude that P700 exhibits a maximum at ~ 702 nm and FWHM of $350\,cm^{-1}$ at 1.6 K. From our theoretical analysis approximately 30 and 70% of this width is due to inhomogeneous broadening and homogeneous broadening (from linear electron–phonon coupling), respectively.

In our laboratory we have now studied the spectral hole burning of the PED states P680* of PS II (Jankowiak et al. 1989), P700* of PS I (Gillie et al. 1987a, this work), P870* of *Rb. sphaeroides* (Johnson et al. accepted, Tang et al. accepted) and P960* of *Rps. viridis* (Tang et al. 1988, Tang et al. 1989). It is appropriate, therefore, to compare the hole spectra for these systems. The crystal structures for the RC of *Rb. sphaeroides* (Allen et al. 1986, Chang et al. 1986) and *Rps. viridis* (Deisenhofer et al. 1984, Deisenhofer et al. 1985, Michel et al. 1986) have been determined and the structural

arrangements for the special pair, two monomer BChl and two BPheo (bacteriopheophytin) are very similar (Allen et al. 1987a). The RC structures for PS I and PS II have not been determined. However, the RC of PS II appears to share structural and functional similarities with the RC of the purple bacteria (Michel and Deisenhofer 1986, Trebst 1986, Michel and Deisenhofer 1987) and the Nanba–Satoh preparation (Nanba and Satoh 1987) of the PS II RC binds 4–5 Chl *a* and two Pheo *a* molecules. Our studies of P960 (Tang et al. 1988,. Tang et al. 1989) which utilized several different glass-detergent hosts, revealed that the hole spectrum is comprised of several relatively broad holes including a vibronic hole of $\sim 130\,cm^{-1}$ that builds on the lowest energy hole denoted as X. A study of the λ_B-dependence of the hole structure established that it is intrinsic to a single active RC and not due to gross heterogeniety or impurity. Very recently the experiments were repeated (Tang et al. accepted, Johnson et al. accepted) using redissolved *Rps. viridis* crystals of the quality used for crystallographic studies. Spectra (both Δ-absorbance and -transmisison) were obtained that allow for better characterization of the structure reported earlier. For example, higher progression members of the $\sim 130\,cm^{-1}$ mode were observed in the hole spectra. Experiments have also been completed in which redissolved crystals of *Rb. sphaeroides* were used (Johnson et al. accepted, Tang et al. accepted). Importantly, the hole structure observed for P960 is also observed for P870. For both P870 and P960 a weak ZPH is observed superimposed on hole X when λ_B is located in the region corresponding to the absorption that is associated with hole X. The widths of the ZPH yield decay times that are in agreement with those determined for P870* and P960* at 10 K by ultra-fast spectroscopy (Martin et al. 1986, Breton et al. 1988).

The progression forming $\sim 130\,cm^{-1}$ mode plays an important role in determination of the hole structure to higher energy of X for P870 and P960. Interestingly, the P680 hole profile (Jankowiak et al. 1989, see Fig. 1), appears to be quite similar to the X hole and ZPH for P870. However, the studies on P680 have failed to reveal the presence of satellite hole structure due to a $\sim 130\,cm^{-1}$ mode (Jankowiak et al. 1989). This mode has been assigned as an intermolecular special pair marker mode (Johnson et al. accepted, Tang et al. accepted) and, thus, its apparent absence could be relevant to the question of the existence of the special pair or its structure (if it does exist).

From the above brief overview and the results presented here for P700 it is apparent that the P700 hole spectra are significantly different from those for the other PED states. Although there appear to be significant differences (Allen et al. 1988, Yeates et al. 1988) between the interactions of the special pair and amino acid residues in *Rps. viridis* and *Rb. sphaeroides* the similarity in their cofactor structures (Allen et al. 1987a, Allen et al. 1987b) is sufficient to yield very similar hole spectra for P960 and P870. The hole spectra for P700 show no evidence of any structure (akin to that associated with the $\sim 130\,cm^{-1}$ mode of P870 and P960) even though the P700 hole profile and calculated absorption profile are about $100\,cm^{-1}$ narrower than the overall hole widths and absorption widths of P870 and P960. This, together with the fact that $\Gamma_I \sim 100\,cm^{-1}$ for P700, is telling in the sense that if a mode analogous to the $\sim 130\,cm^{-1}$ is active in the P700 hole profile, the fact that it cannot be resolved means that its frequency and/or Franck–Condon factor are considerably reduced. We cannot distinguish between this possibility or the possibility that such a progression forming mode does not exist. The existence of the special pair for P700 is still being debated but evidence for its existence appears to be mounting (Golbeck 1989). Assuming that it does exist, the above remarks and the absence of the ZPH for P700 indicate that its geometric and/or its excited state electronic structure might be quite different than for the purple bacteria.

Finally, we note that it should be possible to simulate the unstructured hole spectra reported here for P700 by reducing the linear electron–phonon coupling strength and compensating for this reduction by introducing an ultra-fast electronic relaxation channel for P700*. The theory of Won and Friesner 1988a would be appropriate for such simulations.

5. Conclusions

The P700 hole profiles obtained for a wide range of burn wavelegnths λ_B do not exhibit a sharp ZPH coincident with λ_B, are broad ($\sim 310\,cm^{-1}$) and devoid of structure due to low frequency Chl *a* intramolecular modes or inter-pigment modes.

They provide an interesting contrast with the hole profiles for the PED states of other RC. The P700 hole profiles, with their modest λ_B-dependence, can be modeled using the theory of Hayes and Small (1986). In so doing it is estimated that 30% of the P700 absorption width ($\sim 350\,cm^{-1}$) is due to inhomogeneous broadening arising from slight structural variations from RC to RC and 70% to homogeneous broadening. The theory ascribes the latter broadening to linear electron–phonon coupling and not to ultra-fast electronic relaxation of P700*. Inclusion of two different mean phonon frequencies in the theoretical analysis would not markedly change the above percentages. The theoretical analysis yields a value of ~ 710 nm for the location of the zero-point level of P700* at 1.6 K. The P700 absorption profile maximum occurs at ~ 702 nm with the differences between this wavelength and 710 nm due to the reorganization energy ($S\omega_m$) associated with the optical excitation. The strong linear electron–phonon coupling for P700* suggests that it may possess significant charge-transfer character as appears to be the case for P870* (Braun et al. 1987, Lockhart and Boxer 1987, Lösche et al. 1987, Lockhart and Boxer 1988) and P960* (Braun et al. 1987, Lösche et al. 1987, Lockhart and Boxer 1988).

Acknowledgements

The Ames Laboratory is operated for the U.S. Department of Energy by Iowa State University under contract No. W-7405-ENG-82. The research of J.K.G. and G.J.S. was supported by the Director for Energy Research, Office of Basic Energy Science. The research of J.H.G. was supported by the Cooperative State Research Service, U.S. Department of Agriculture, Agreement No. 87-CRCR-1-2382. We thank D. Tang and R. Jankowiak for providing us with the P680 spectrum shown in Fig. 1.

References

Allen JP, Feher G, Yeates TO, Rees DC, Deisenhofer J, Michel H and Huber R (1986) Structural homology of reaction centers from *Rhodopseudomonas sphaeroides* and *Rhodopseudomonas viridis* as determined by X-ray diffraction. Proc Natl Acad Sci USA 83: 8589–8593

Allen JP, Feher G, Yeates TO, Komiya H and Rees DC (1987a) Structure of the reaction center from *Rhodobacter sphaeroides* R-26: the cofactors. Proc Natl Acad Sci USA 84: 5730–5734

Allen JP, Feher G, Yeates TO, Komiya H and Rees DC (1987b) Structure of the reaction center from *Rhodobacter sphaeroides* R-26: the protein subunits. Proc Natl Acad Sci USA 84: 6161–6166

Allen JP, Feher G, Yeates TO, Komiya H and Rees DC (1988) Structure of the reaction center from *Rhodobacter sphaeroides* R-26: protein-cofactor (quinones and Fe^{2+}) interactions. Proc Natl Sci USA 85: 8487–8491

Bearden AJ and Malkin R (1972) Quantitative EPR studies of the primary reaction of photosystem I in chloroplasts. Biochim Biophys Acta 283: 456–468

Boxer SG, Lockhart DJ and Middendorf TR (1986a) Photochemical hole burning in photosynthetic reaction centers. Chem Phys Lett 123: 476–482

Boxer SG, Middendorf TR and Lockhart DJ (1986b) Reversible photochemical hole burning in *Rhodopseudomonas viridis* reaction centers. FEBS Lett 200: 237–241

Braun HP, Michel-Beyerle ME, Breton J, Buchanan S and Michel H (1987) Electric field effect on absorption spectra of reaction centers of *Rb. sphaeroides* and *Rps. viridis*. FEBS Lett 221: 221–225

Breton J, Martin J-L, Fleming GR and Lambry J-C (1988) Low-temperature femtosecond spectroscopy of the initial steps of electron transfer in reaction centers from photosynthetic purple bacteria. Biochemistry 27: 8276–8284

Chang CH, Tiede D, Tang J, Smith U, Norris J and Schiffer M (1986) Structure of *Rhodopseudomonas sphaeroides* R-26 reaction center. FEBS Lett 205: 82–86

Deisenhofer J, Epp O, Miki K, Huber R and Michel H (1984) X-ray structure analysis of a membrane protein complex: electron density map at 3 Å resolution and a model of the chromophores of the photosynthetic reaction center from *Rhodopseudomonas viridis*. J Mol Biol 180: 385–398

Deisenhofer J, Epp O, Miki K, Huber R and Michel H (1985) Structure of the protein subunits in the photosynthetic reaction center of *Rhodopseudomonas viridis*. Nature (London) 318: 618–624

Fenton JM, Pellin MJ, Govindjee and Kaufmann KJ (1979) Primary photochemistry of the reaction center of photosystem I. FEBS Lett 100: 1–4

Fearey BL, Carter TP and Small GJ (1983) Efficient nonphotochemical hole burning of dye molecules in polymers. J Phys Chem 87: 3590–3592

Friedrich J, Swalen JD and Haarer D (1980) Electron–phonon coupling in amorphous organic host materials as investigated by photochemical hole burning. J Phys Chem 73: 705–711

Friedrich J and Haarer D (1984) Photochemical hole burning: a spectroscopic study of relaxation processes in polymers and glasses. Angew Chem Int Ed Engl 23: 113–140

Gillie JK, Fearey BL, Hayes JM, Small GJ and Golbeck JH (1987a) Persistent hole burning of the primary donor state of photosystem I: strong linear electron–phonon coupling. Chem Phys Lett 134: 316–322

Gillie JK, Hayes JM, Small GJ and Golbeck JH (1987b) Hole burning spectroscopy of a core antenna complex. J Phys Chem 91: 5524–5527

Gillie JK, Small GJ and Golbeck JH (1989) Nonphotochemical hole burning of the native complex of photosystem I (PSI-

200). J Phys Chem 93: 1620–1627
Golbeck JH (1980) Subchloroplast particle enriched in P700 and iron-sulfur protein. In: San Pietro A (ed) Methods in Enzymology, vol 69, pp 129–141. New York: Academic Press
Golbeck JH (1987) Structure, function, and organization of the Photosystem I reaction center complex. Biochim Biophys Acta 895: 167–204
Hayes JM and Small GJ (1986) Photochemical hole burning and strong electron–phonon coupling: primary donor states of reaction centers of photosynthetic bacteria. J Phys Chem 90: 4928–4931
Hayes JM, Gillie JK, Tang DT and Small GJ (1988) Theory for spectral hole burning of the primary electron donor state of photosynthetic reaction centers. Biochim Biophys Acta 932: 287–305
Hayes JM and Small GJ (1978) Nonphotochemical hole burning and impurity site relaxation processes in organic glasses. Chem Phys 27: 151–157
Jankowiak R, Tang D, Small GJ and Seibert M (1989) Transient and persistent hole burning of the reaction center of photosystem II. J Phys Chem 93: 1649–1654
Jankowiak R and Small GJ (1987a) Hole burning spectroscopy and relaxation dynamics of amorphous solids at low temperatures. Science 237: 618–625
Jankowiak R, Shu L, Kenney MJ and Small GJ (1987b) Dispersive kinetic processes, optical linewidths and dephasing in amorphous solids. J Lumin 36: 293–305
Johnson SG and Small GJ (1989) Spectral hole burning of a strongly excitonic coupled bacteriochlorophyll *a* antenna complex. Chem Phys Lett 155: 371–375
Johnson SG, Tang D, Jankowiak R, Hayes JM, Small GJ and Tiede, DM (accepted) Structure and marker mode of the primary electron donor state absorption of photosynthetic bacteria: hole burned spectra. J Phys Chem
Ke B, Demeter S, Zamaraea KI and Khairutdimov RF (1978) Charge recombination in photosystem I at low temperatures. Biochim Biophys Acta 545: 265–284
Köhler W, Friedrich J, Fischer R and Scheer H (1988a) Site-selective spectroscopy and level ordering in c-phycocyanine. Chem Phys Lett 143: 169–173
Köhler W, Friedrich J, Fischer R and Scheer H (1988b) High resolution frequency selective photochemistry of phycobilisomes at cryogenic temperatures. J Chem Phys 89: 871–874
Lee IJ, Hayes JM and Small GJ (accepted) Hole and anti-hole profiles in non-photochemical hole burned spectra. J Chem Phys
Lockhart DJ and Boxer SG (1987) Magnitude and direction of the change in dipole moment associated with excitation of the primary electron donor in *Rhodopseudomonas sphaeroides* reaction centers. Biochemistry 26: 664–668
Lockhart DJ and Boxer SG (1988) Stark effect spectroscopy of *Rhodobacter sphaeroides* and *Rhodopseudomonas viridis* reaction centers. Proc Natl Acad Sci USA 85: 107–111
Lösche M, Feher G and Okamura MY (1987) The stark effect in reaction centers from *Rhodobacter sphaeroides* R-26 and *Rhodopseudomonas viridis*. Proc Natl Acad Sci USA 84: 7537–7541
Martin J-L, Breton J, Hoff AJ, Migus A and Antonetti A (1986) Femtosecond spectroscopy of electron transfer in the reaction center of the photosynthetic bacterium *Rhodopseudomonas sphaeroides* R-26: direct electron transfer from the dimeric bacteriochlorophyll primary donor to the bacteriopheophytin acceptor with a time constant of 2.8 ± 0.2 ps. Proc Natl Acad Sci USA 83: 957–961
Meech SR, Hoff AJ and Wiersma DA (1985) Evidence for a very early intermediate in bacterial photosynthesis. A photon-echo and hole-burning study of the primary donor band in *Rhodopseudomonas sphaeroides*. Chem Phys Lett 121: 287–292
Meech SR, Hoff AJ and Wiersma DA (1986) Role of charge-transfer states in bacterial photosynthesis. Proc Natl Acad Sci USA 83: 9464–9468
Michel H, Epp O and Deisenhofer J (1986) Pigment–protein interactions in the photosynthetic reaction center from *Rhodopseudomonas viridis*. EMBO J 5: 2445–2451
Michel H and Deisenhofer P (1986) X-ray diffraction studies on a crystalline bacterial photosynthetic reaction center: a progress report and conclusions on the structure of photosystem II reaction centers. In: Staehelin AC and Arntzen CJ (eds) Encylopedia of Plant Physiology: Photosynthesis III, pp 371–381. Berlin: Springer-Verlag
Michel H and Deisenhofer J (1987) The photosynthetic reaction center from the purple bacterium *Rhodopseudomonas viridis*. Chemica Scripta 27B: 173–180
Moerner WE (ed) (1988) Persistent spectral hole-burning: science and applications. Berlin: Springer-Verlag
Mullet JE, Burke JJ, Arntzen CJ (1980) Chlorophyll proteins of Photosystem I. Plant Physiol 65: 814–822
Nanba O and Satoh K (1987) Isolation of a photosystem II reaction center consisting of D-1 and D-2 polypeptides and cytochrome *b*-559. Proc Natl Acad Sci USA 84: 109–112
Owens TG, Webb SP, Mets L, Alberts RS and Fleming GR (1987) Antenna size dependence of fluorescence decay in the core antenna of photosystem I: estimates of charge separation and energy transfer rates. Proc Natl Acad Sci USA 84: 1532–1536
Renge I, Mauring K and Avarmaa R (1987) Site-selection optical spectra of bacteriochlorophyll and bacteriopheophytin in frozen solutions. J Lumin 37: 207–214
Renge I, Mauring K and Vladkova R (1988) Zero-phonon transitions of chlorophyll *a* in mature plant leaves revealed by spectral hole-burning method at 5 K. Biochim Biophys Acta 935: 333–336
Schaffernicht H and Junge W (1981) Analysis of the complex band spectrum of P700 based on photoselection studies with photosystem I particles. Photochem Photobiol 34: 223–232
Sétif P, Mathis P and Vänngård T (1984) Photosytem I photochemistry at low temperature: heterogeniety in pathways for electron transfer to the secondary acceptors and for recombination processes. Biochim Biophys Acta 767: 404–414
Small GJ (1983) Persistent nonphotochemical hole burning and the dephasing of impurity electronic transitions in organic glasses. In: Agranovich VM and Hochstrasser RM (eds) Spectroscopy and excitation dynamics of condensed molecular systems, pp 515–554. Amsterdam: North-Holland
Small GJ (1970) Multiplet and phonon structure in mixed crystal spectra: anthacene in p-terphenyl. J Chem Phys 52: 656–673
Tang D, Jankowiak R, Gillie JK, Small GJ and Tiede DM (1988) Structured hole-burned spectra of reaction centers of

Rhodopseudomonas viridis. J Phys Chem 92: 4012–4015

Tang D, Jankowiak R, Small GJ and Tiede DM (1989) Structured hole-burned spectra of the primary donor state absorption region of *Rhodopseudomonas viridis*. Chem Phys 131: 99–113

Tang D, Johnson SG, Jankowiak RJ, Hayes JM, Small GJ and Tiede DM (accepted) Structure and marker mode of the primary electron donor state absorption of photosynthetic bacteria: hole burned spectra. In: Jortner J and Pullman B (eds) Twenty-Second Jerusalem Symposium Quantum Chemistry and Biochemistry: Perspectives in Photosynthesis. Kluwer Academic: Dordrecht, to be published

Trebst A (1986) The topology of the plastoquinone and herbicide binding peptides of photosystem II in the thylakoid membrane. Z Naturforsch 41C: 240–245

Wasielewski MR, Johnson DG, Seibert M and Govindjee (1989) Determination of the primary charge separation rate in isolated photosystem II reaction centers with 500-fs time resolution. Proc Natl Acad Sci USA 86: 524–528

Wasielewski MR, Fenton JM and Govindjee (1987) The rate of formation of $P700^+$–A_0^- in photosystem I particles from spinach as measured by picosecond transient absorption spectroscopy. Photosyn Res 12: 181–190

Won Y and Friesner RA (1988a) Theoretical studies of photochemical hole burning in photosynthetic bacterial reaction centers. J Phys Chem 92: 2214–2219

Won Y and Friesner RA (1988b) On the viability of the superexchange mechanism in the primary charge separation step of bacterial photosynthesis. Biochim Biophys Acta 935: 9–18

Won Y and Friesner RA (1989) Comment: theoretical studies of photochemical hole burning in photosynthetic bacterial reaction centers. J Phys Chem 93: 1007

Yeates TO, Komiya H, Chirino A, Rees DC, Allen JP and Feher G (1988) Structure of the reaction center from *Rhodobacter sphaeroides* R-26 and 2.4.1:protein-cofactor (bacteriochlorophyll, bacteriopheophytin, and carotenoid) interactions. Proc Natl Acad Sci USA 85: 7993–7997